

# A new transfer-matrix algorithm for exact enumerations: Self-avoiding polygons on the square lattice

Nathan Clisby and Iwan Jensen

ARC Centre of Excellence for Mathematics and Statistics of Complex Systems, Department of Mathematics and Statistics, The University of Melbourne, VIC 3010, Australia

**Abstract.** We present a new and more efficient implementation of transfer-matrix methods for exact enumerations of lattice objects. The new method is illustrated by an application to the enumeration of self-avoiding polygons on the square lattice. A detailed comparison with the previous best algorithm shows significant improvement in the running time of the algorithm. The new algorithm is used to extend the enumeration of polygons to length 130 from the previous record of 110.

## 1. Introduction

An  $n$ -step *self-avoiding polygon* (SAP)  $\omega$  on a regular lattice is a sequence of *distinct* vertices  $\omega_0, \omega_1, \dots, \omega_n$  such that each vertex is a nearest neighbour of its predecessor and  $\omega_0$  and  $\omega_n$  are nearest-neighbours. SAP are considered distinct up to translations of the starting point  $\omega_0$  and orientation. The SAP problem on regular lattices is one of the most important and classic combinatorial problems in statistical mechanics [1, 2, 3]. SAP are often considered in the context of lattice models of ring-polymers and vesicles [4, 5, 6]. The fundamental problem is the calculation of the number of SAP,  $p_n$ , with  $n$  steps. Note that on the square lattice polygons have an *even* perimeter and  $p_n = 0$  for  $n$  odd. As most interesting combinatorial problems, SAP have exponential growth

$$p_n = B\mu^n n^{\alpha-3}[1 + o(1)], \quad (1)$$

where  $\mu$  is the so-called connective constant,  $\alpha = 1/2$  is a (known) universal critical exponent [7, 8], and  $B$  is a critical amplitude. When analysing the data it is often convenient to use the associated generating function

$$P(x) = \sum_n p_n x^n = \hat{B}(x)(1 - x\mu)^{2-\alpha}. \quad (2)$$

This series has a singularity at the critical point  $x_c = 1/\mu$  with critical exponent  $2 - \alpha$ .

The enumeration of SAP has a long and glorious history. Suffice to say that early calculations were based on various direct counting algorithms of exponential complexity, with computing time  $T(n)$  growing asymptotically as  $\lambda^n$ , where  $\lambda = \mu \sim 2.638$ , the

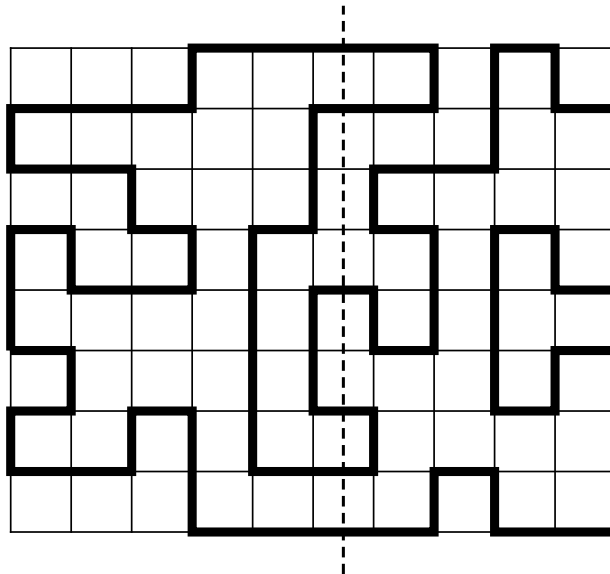


**Figure 1.** An example of a SAP on a  $10 \times 8$  rectangular piece of the square lattice. The dashed line shows a position of the TM boundary at a particular stage of the calculation.

connective constant for SAP on the square lattice. Enting [9] was the first to produce a major breakthrough by applying transfer matrix (TM) methods to the enumeration of SAP on finite lattices. This so-called finite lattice method (FLM) led to a very significant reduction in complexity to  $3^{n/4}$ , so  $\lambda = \sqrt[4]{3} = 1.316\dots$ . More recently we [10] refined the algorithm using the method of pruning and reduced the complexity to  $1.2^n$ .

All of the above TM algorithms are based on keeping track of the way partially constructed SAP are connected to the left of a line bisecting the given finite lattice (rectangles in the case of the square lattice). In this paper we take a new approach and instead keep track of how partially constructed SAP must connect up to the right of the boundary line. The major gain is that it is now straightforward to calculate the number additional bonds required to complete a given partial SAP, this in turn results in a substantially faster algorithm. The draw-back is that some updating rules become much more complicated. The basic idea can best be illustrated by considering the specific example of a SAP given in Figure 1. If we cut the SAP by a vertical line (the dashed line) we see that the SAP is broken into two pieces to the left and right of the cut-line. On *either* side of the line we are left with a set of partial loops. This means that at any stage a given configuration of occupied edges along the cut-line can be described in two ways. We can describe how the edges are connected in pairs forming loops to the left or right of the cut-line. Moving from left to right we can in other words keep track of what happened in the past, that is how loops are connected to the left, or prescribe what must happen in the future, that is how edges are to be connected to the right of the cut-line so as to form a valid SAP.

One may think of the new FLM method as taking an initial seed SAP which must touch the left hand boundary of the enclosing rectangle. Here there is a known part consisting of two edges to the left of the boundary line, and to the right of the boundary line a self-avoiding walk of known topology but unknown shape and length. As the boundary line is moved through the lattice the overall topology of the SAP must be preserved, but the topology of the configuration on the right hand side of the boundary line may be deformed. The restriction in the extent to which the topology can be deformed is a consequence of the choice in updates for the boundary line, which for the square lattice only moves to enclose one additional vertex and two additional edges in each update.

This picture of the new FLM method is equally applicable to the enumeration of any lattice object with fixed topology, such as self-avoiding walks, theta graphs [11], or star polymers.

## 2. The finite-lattice method and TM algorithms

All TM algorithms used to enumerate SAP on the square lattice build on the pioneering work of Enting [9] who enumerated square lattice self-avoiding polygons using the finite lattice method. The first terms in the series for the polygon generating function can be calculated using transfer matrix techniques to count the number of polygons in rectangles  $W$  vertices wide and  $L$  vertices long. Due to the symmetry of the square lattice one need only consider rectangles with  $L \geq W$ . Any polygon spanning such a rectangle has a perimeter of length at least  $2(W + L) - 4$ . By adding the contributions from all rectangles of width  $W \leq W_{\max}$  (where the choice of  $W_{\max}$  depends on available computational resources) and length  $W \leq L \leq 2W_{\max} - W + 1$ , with contributions from rectangles with  $L > W$  counted twice, the number of polygons per vertex of an infinite lattice is obtained correctly up to perimeter  $N = 4W_{\max} - 2$ .

### 2.1. Outline of the traditional TM algorithm

The generating function for a rectangle is calculated using transfer matrix techniques. Details of our previous algorithm can be found in [10, 12] and Chapter 7 of [3]. Here we outline those aspects common to both algorithms that are needed to appreciate the differences. The most efficient implementation of the TM algorithm generally involves bisecting the finite lattice with a boundary and moving the boundary in such a way as to build up the lattice vertex by vertex as illustrated in Figure 2. If we draw a SAP and then cut it by a line we observe that the partial SAP to the left of this line consists of a number of loops connecting two edges (we shall refer to these as loop-ends) in the intersection. Each end of a loop is assigned one of two labels depending on whether it is the lower or upper end of a loop. Each configuration along the boundary line can thus

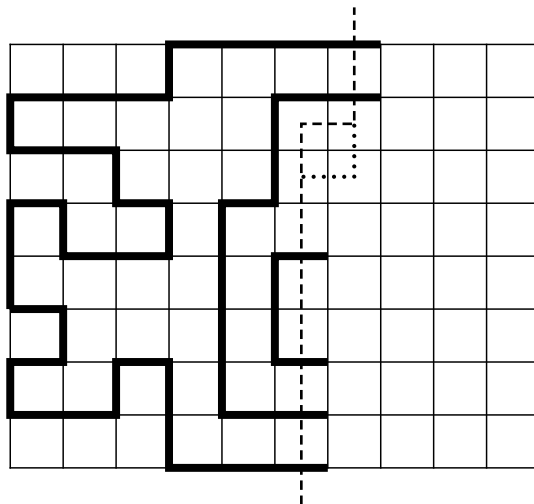


**Figure 2.** A snapshot of the boundary line (dashed line) during the transfer matrix calculation of type *A* configurations on a strip of size  $8 \times 10$ . SAP are enumerated by successive moves of the kink in the boundary line, as exemplified by the position given by the dotted line, so that one vertex and two edges at a time are added to the strip. To the left of the boundary line we have drawn an example of a partially completed SAP.

be represented by a set of edge states  $\{\sigma_i\}$ , where

$$\sigma_i = \begin{cases} 0 & \text{empty edge,} \\ 1 & \text{lower loop-end,} \\ 2 & \text{upper loop-end.} \end{cases} \quad (3)$$

If we read from the bottom to the top, the configuration or signature  $S$  along the intersection of the partial SAP in Figure 2 is  $S = \{1110200022\}$ . Since crossings are not permitted this encoding uniquely describes how the loop-ends are connected.

In applying the transfer matrix technique to the enumeration of polygons we regard them as sets of edges on the finite lattice with the properties:

- (1) A weight  $x$  is associated with each occupied edge.
- (2) All vertices are of degree 0 or 2.
- (3) Apart from isolated sites, the graph has a single connected component.
- (4) Each graph must span the rectangle from left to right and from bottom to top.

Constraint (1) is trivial to satisfy. The sum over all contributing graphs (valid SAP) is calculated as the boundary is moved through the lattice. For each configuration of occupied or empty edges along the intersection we maintain a generating function  $G_S$  for partial polygons with signature  $S$ . In exact enumeration studies  $G_S$  is a truncated polynomial  $G_S(x)$  where  $x$  is conjugate to the number of occupied edges. In a TM update each source signature  $S$  (before the boundary is moved) gives rise to one or two new target signatures  $S'$  (after the move of the boundary line) and  $k = 0, 1$  or  $2$  new edges are inserted leading to the update  $G_{S'}(x) = G_S(x) + x^k G_S(x)$ .

Constraint (2) is easy to satisfy. If both kink edges are empty we can leave both new edges empty or insert a partial new loop by occupying both of the new edges. If one of the kink edges is occupied then one of the new edges must also be occupied. If both of the kink edges are occupied both of the new edges must be empty. It is easy to see that these rules leads to graphs satisfying constraint (2).

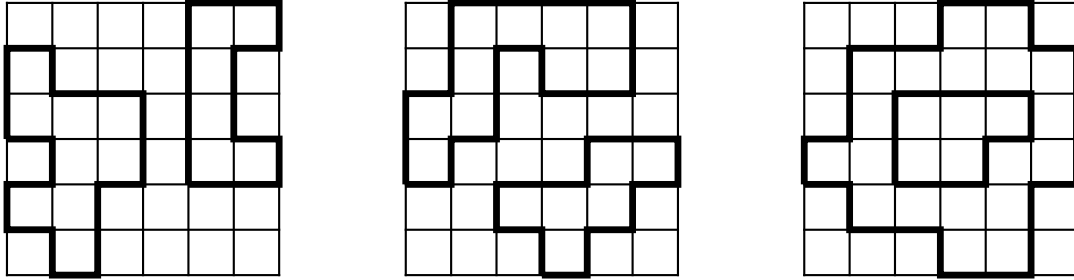


**Figure 3.** Three ways in which graphs with separate components could occur.

Constraint (3) is the most difficult to satisfy. We have shown some examples of two-component graphs in Figure 3. Graphs of the type shown in the left-most panel, where separate components occur side by side, are quite easy to avoid by never allowing the insertion of a new loop into the totally empty configuration except for the initial seed state. This also ensures that all polygons touch the left-most border of the rectangle. There are only two distinct ways in which a pair of loops can be placed relative to one another – side by side or nested – as shown in the last two panels of Figure 3. With the loop encoding given above multiple components are avoided by not allowing two connected loop-ends to join *except* when no other loop-ends are present in which case a completed SAP is formed.

In order to satisfy constraint (4) we need to add more information to a signature. In addition to the usual labelling of the intersection with the boundary line we also have to indicate whether the partially completed polygon has reached neither, both, the lower, or the upper boundaries of the rectangle. In order to represent a given partial polygon we have to add some information to the usual set of edge states  $\{\sigma_i\}$ . We add two extra ‘virtual’ edge states  $\sigma_b$  and  $\sigma_t$ , where  $\sigma_b$  is 0 or 1 if the bottom of the rectangle has or has not been touched. Similarly,  $\sigma_t$  is 0 or 1 if the top of rectangle has or has not been touched.

## 2.2. The new algorithm

Most of the basic properties and considerations outlined in the previous Section apply also to the new algorithm. A major difference is conceptual namely that as stated in Section 1 we change the way we keep track of the partial loops intersecting the boundary line. While we can use exactly the same encoding of a signature as (3) the meaning of ‘lower’ and ‘upper’ loop-end is profoundly different. In the original algorithm these terms referred to partial loops connected to the left of the boundary, that is, to how the

existing loops in the partially generated SAP are already connected. However, in the new algorithm ‘lower’ and ‘upper’ loop-end refers to how occupied edges along the boundary must be connected via a loop at some later stage (to the right of the boundary). This change in turn results in new updating rules for the cases where a new loop is inserted or two loop-ends join at the kink. We deal with the latter easier modification first.

We can join two loop-ends at the boundary kink *only* if they belong to the same loop, thus closing a partial loop of the SAP, since the loop encoding of new algorithm simply prescribes how occupied edges are to be connected. Thus the only valid case is the kink-state ‘12’ and all the other kink states (‘11’, ‘22’ and ‘21’) are forbidden since they would correspond to connecting occupied edges which should not have been connected. Two situations arise when a partial loop is closed; *either* there are other occupied edges along the boundary and one just proceeds with the calculation or all other edges are empty and a closed SAP is formed and added to the running total for the SAP generating function.

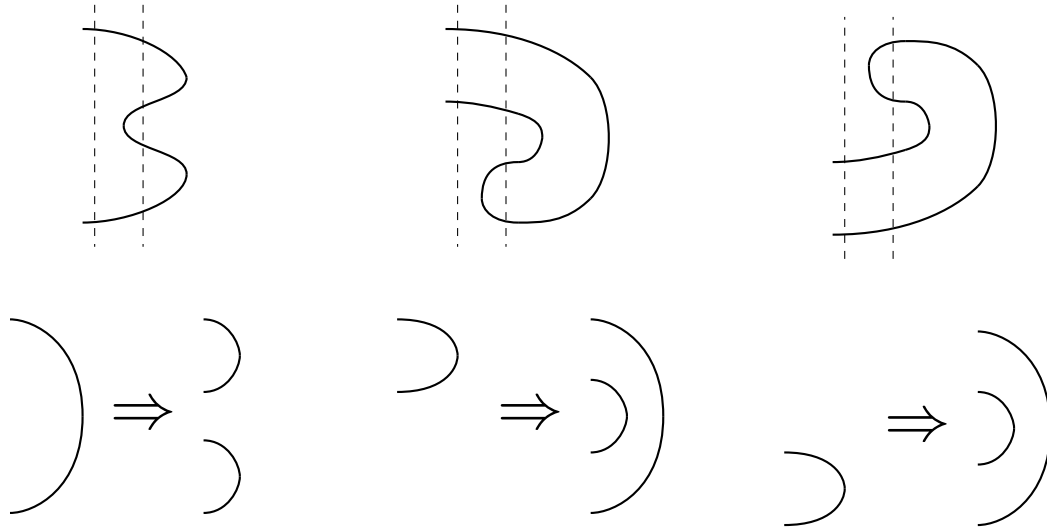


**Figure 4.** The possible basic deformations to the topology of a boundary state as the boundary line is shifted are shown schematically above. The corresponding basic loop updates are shown immediately below.

While edge-joining is simplified the insertion of a new loop becomes much more complicated. In the original approach the insertion was done and no further action was required. In the new approach we must connect the two new occupied edges to other occupied edges on the boundary line. The restrictions on SAP enumeration mean that the two new occupied edges must connect to existing *connected edges* provided these are reachable (more on this later). The state of the new occupied edges will depend on their placement relative to the edges they become connected to, and the state of the existing occupied edges may change. In Figure 4 we show the two basic situations: The new occupied edges are either placed inside the loop formed by the two existing connected edges or they are placed outside them. In the first case, shown to the left in Figure 4,

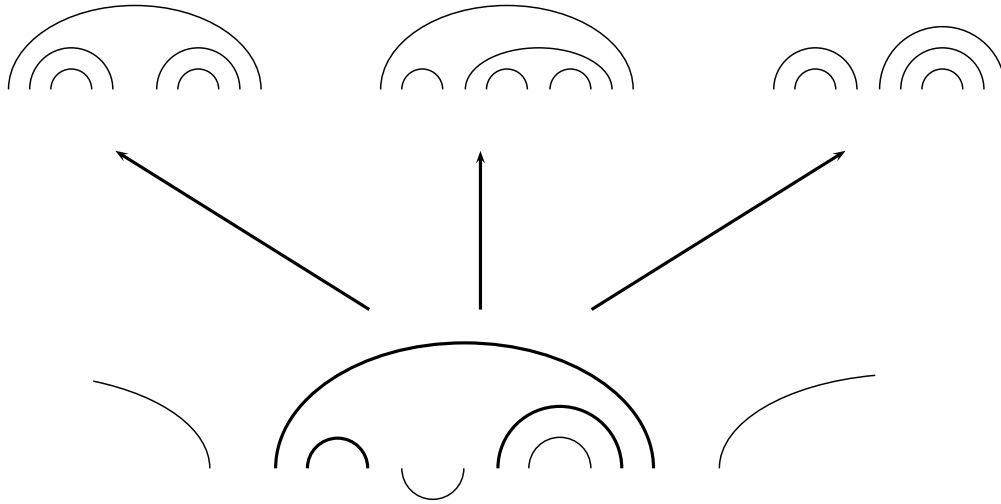


**Figure 5.** The possible updates resulting from the insertion of a new partial loop into an existing loop configuration. At the bottom we indicate by a lower arc the new partial loop. In the existing loop configuration (upper arcs) accessible loops are indicated with heavy lines. The three possible new loop configurations are shown on top.

the upper (lower) end of the inserted loop must connect with the upper (lower) end of the existing loop, in terms of the edges involved the states change from ‘1002’ to ‘1212’. In the second case, in the middle of the figure, the upper (lower) end of the inserted loop must connect with the lower (upper) end of the existing loop, in terms of the edges involved the states change from ‘1200’ to ‘1122’. So *both* new occupied edges become ‘lower’ loop-ends while the existing lower loop-end is changed to an upper loop-end. Shown to the right in Figure 4, there is also a symmetric case where the new loop is placed above the existing loop leading to the state change ‘0012’ to ‘1122’.

The newly inserted loop can connect to any existing loop that can be reached without crossing another loop. The general situation is illustrated in Figure 5 where we see that the new loop can be connected to three existing loops (indicated by thick lines). The second loop to the right of the new loop is nested inside an existing loop and can therefore *not* be reached without crossing the enclosing loop. Likewise any loops outside the large loop enclosing the new loop are unreachable. So in this case the insertion of a single new loop gives rise to three new loop configurations as illustrated in the top panels of Figure 5. The states of the edges in the new loop configurations are obtained by applying the appropriate basic loop insertion from above.

At this stage it seems nothing has been gained. Some updates simplify while loop-insertion becomes much more complicated. The true pay-off comes when we look to pruning. In the original approach pruning can be very complicated. With deeply nested configurations one simply has to search through all possible ways of connecting existing partial loops in order to find the connection pattern which minimises the number of extra edges required to form a valid SAP. In the new approach this complication is

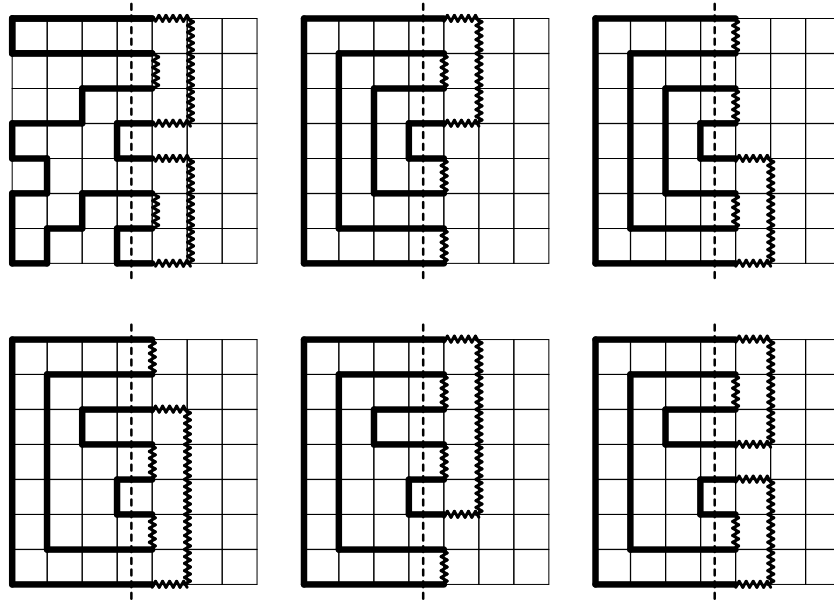


**Figure 6.** Examples of partially generated polygons (thick solid lines) to the left of the intersection (dashed line) and how to close them in a valid way (thick wavy line). Upper left panel shows how to close the configuration  $\{12112212\}$ . The upper middle and right panels show the two possible closures of the configuration  $\{11112222\}$ . The lower panels show the three possible closures of the configuration  $\{11121222\}$ .

completely gone since connections between edges is already prescribed: There is one and only one way of completing the SAP!

### 2.3. Pruning

The principle behind pruning is quite simple and briefly works as follows. Firstly, for each signature we keep track of the current minimum number of steps  $n_{\text{cur}}$  already inserted to the left of the boundary line in order to build up that particular configuration. Secondly, we calculate the minimum number of additional steps  $n_{\text{add}}$  required to produce a valid polygon. There are three contributions, namely the number of steps required to close the polygon, the number of steps needed (if any) to ensure that the polygon touches both the lower and upper border, and finally the number of steps needed (if any) to extend at least  $W$  edges in the length-wise direction (remember we only need rectangles with  $L \geq W$ ). If the sum  $n_{\text{cur}} + n_{\text{add}} > N = 4W_{\text{max}} + 2$  we can discard the partial generating function for that configuration, and of course the configuration itself, because it will not make a contribution to the polygon count up to the perimeter lengths we are trying to obtain. For instance polygons spanning a rectangle with a width close to  $W_{\text{max}}$  have to be almost convex, so very convoluted polygons are not possible. Thus configurations with many loop-ends (non-zero entries) make no contribution at perimeter length  $\leq N$ .

The complicated part of the pruning approach is the algorithm to calculate the



number of steps required to close the polygon. In the first stage we connect any separate pieces as illustrated in Figure 6. Separate pieces are easy to locate and (provided one is not at the last edge in the configuration) the top-most upper edge of one piece can be connected to the lower edge above. Then  $n_{\text{add}}$  is incremented by the number of steps (the distance) between the edges and the two edge-states are removed from the configuration before further processing. In the second stage we transform configurations starting (ending) as  $\{112 \dots 2\}$  ( $\{1 \dots 122\}$ ) since the two lower (upper) edges can safely be connected. The two edge-states are removed from the configuration – leading to the new configuration  $\{001 \dots 2\}$  ( $\{1 \dots 200\}$ ) – before further processing.

After these two stages we may be left with a configuration which has just a single lower edge and a single upper edge. We are almost done since these two edges can be connected to form a valid polygon. This is illustrated in Figure 6 where the upper left panel shows how to close the partial polygon with the intersection  $\{12112212\}$ , which contain three separate pieces. After connecting these pieces we are left with the configuration  $\{10012002\}$ . We now connect the two lower edges and note that the first upper edge is relabeled as a lower-edge (it has become the new lower end of the loop). Thus we get the configuration  $\{00001002\}$  and we can now connect the remaining two edges and end up with a valid completed polygon. Note that in the last two cases, in addition to the steps spanning the distance between the edges, an additional two horizontal steps had to be added in order to form a valid loop around the intervening edges.

If the transformations above do not result in a closed polygon we must have a configuration of the form  $\{111 \dots 222\}$ . The difficulty lies in finding the way to close such configurations with the smallest possible number of additional steps. Suffice to say that if the number of non-zero entries is small one can easily code all possible valid ways of closing a polygon and thus find the minimum number of additional steps. In Figure 6 we show all possible ways of closing polygons with 8 non-zero entries. Note that we have shown the generic cases here. In actual cases there could be any number of empty edges interspersed in the configurations and this would determine which way of closing the SAP would minimise  $n_{\text{add}}$ . The number of distinct configurations are given by the Catalan numbers so there is only 1 configuration with 6 occupied edges, while there are 2 with 8 occupied edges, and 5 with 10 occupied edges. In [12] the various possible ways of closing all such configurations was hand-coded. In the more general case (configurations with 12 or more non-empty entries) we devised a basic search algorithm that simply tried all possible ways of closing loops. In practise initially two loop-ends are connected. The resulting new configuration is passed through the two stages above and we are left with a configuration with at least two fewer loop-ends. If there are still open loops we do another pass and so on until all loops have been closed. This process is then repeated but starting with a different pair of initial edges. In this way one can search through all possible ways of completing a SAP. Obviously one would expect that this process should ultimately grow exponentially with the number of non-zero edges. However, due to the simplifying feature of passing through the first two stages

the growth is quite slow.

In the new approach almost all of the complications of pruning are gone. Since connections between edges are already prescribed there is one and only one way of completing the SAP! The only complicating factor is that in order to calculate  $n_{\text{add}}$  we need to know the nesting level  $l$  of each partial loop. The number of edges it takes to connect two loop-ends at positions  $i$  and  $j$  is simply  $j - i + 2l$ . In addition we must connect to the lower and upper boundaries and ensure that the SAP extends at least  $W$  edges in the length-wise direction. This pruning procedure can be performed in  $O(W)$  operations.

#### 2.4. Comparative study of the algorithms

In analysing the complexity of the two algorithms, we note that the update step when the boundary is moved may result in  $O(1)$  signatures for the previous algorithm, and  $O(W)$  for the new one. However, in the average case we still expect the new algorithm to create  $O(1)$  signatures, because connections with distant loop-ends are typically pruned away.

For pruning, we believe that the complexity of the old algorithm is exponential in  $W$  (as we will see below, the growth constant is mercifully small for SAP), whereas for the new algorithm the complexity is  $O(W)$ .

In Table 1 we compare the resources used by the two algorithms in a calculation of the number of SAP with perimeter up to  $N$ . From this it is clear that the new approach is more efficient with substantial savings in time. The required number of configurations and terms go down very slightly while the total CPU time decrease by about 16% for  $N = 98$ . There is little variation in this for the listed values of  $N$ . For higher values of  $N$  we expect to eventually see even more substantial savings in time. As  $N$  increases more deeply nested configurations occur and these are more expensive to prune in the old algorithm. That we do not see an increasing time saving yet is testament to the special nature of square lattice SAP making pruning particularly simple for this problem, and the effort put into the original implementation of pruning for this case. We mention in passing that a preliminary implementation for self-avoiding walks have yielded more substantial time savings of more than 60% for the square lattice.

For large enough  $N$ , we expect the exponential complexity of pruning to make the old algorithm prohibitively slow compared to the new one. However, in practice, for conceivably achievable values of  $N$ , the relative advantage of the new algorithm over the old for the enumeration of SAP may best be described as significant rather than dramatic. For problems where the growth constant for pruning is large, the new algorithm would make a dramatic difference. Candidate problems for potentially dramatic improvement will be mentioned in Section 5.

Finally we mention that due to the simplified joining of loops at the kink (only the ‘12’ case is permitted) it is possible to further improve the algorithm. Since all edges are equivalent we can simplify the kink states to only consider the four possibilities ‘00’, ‘10’,

**Table 1.** A comparison of the resources required by the two algorithms in order to calculate the number of SAP up to length  $N$ .

	Old Algorithm			New Algorithm		
$N$	Configs	Terms	Time	Configs	Terms	Time
42	3837	8275	0.31	3826	8039	0.23
50	15867	37389	2.16	15821	36660	1.63
58	61361	159938	14.60	59354	157367	10.75
66	293853	674548	95.89	286441	652805	78.58
74	1274667	3038260	685.41	1255436	2948937	571.24
82	4973585	12976379	4447.89	4921788	12699279	3783.83
90	22041519	56510740	26770.16	21427764	54845786	22360.05
98	94861519	251027714	173408.04	93020737	244009381	145454.72

‘20’ and ‘12’. That is the vertical edge is only occupied if it is part of a loop joining at the kink. Technically one can also view this as replacing the two kink edges by a vertex with four possible states. The overall net benefit is a drop in memory use by about 15% and a further improvement in running time to a net overall gain of some 30%. This change also simplifies the pruning since a number of special cases (the vertical kink edge being occupied) are avoided. Note however that this change is not always permitted, i.e., on lattices with directed edges (such as the Manhattan or  $L$  lattices) the edges are equivalent and the kink-state simplification isn’t valid.

### 3. Extended SAP enumeration

The transfer-matrix algorithm is eminently suited to parallel computations and here we used the approach first described in [12] to extend the enumeration to SAP of perimeter 130 (that is we obtain a further 10 non-zero terms). The bulk of the calculations for this paper were performed on the cluster of the NCI National Facility at ANU. The NCI peak facility is a Sun Constellation Cluster with 1492 nodes in Sun X6275 blades, each containing two quad-core 2.93GHz Intel Nehalem CPUs with most nodes having 3GB of memory per core (24GB per node). It took a total of about 25000 CPU hours to enumerate SAP up to perimeter 130. We used up to 1000 processors (or more accurately cores) and up to 2.5TB of memory. Some details of resource use are given below.

The integer coefficients occurring in the series expansion become very large and the calculation was therefore performed using modular arithmetic and the series was calculated modulo various integers  $m_i$  and then reconstructed at the end using the Chinese remainder theorem. We used the moduli  $m_0 = 2^{62}$ ,  $m_1 = 2^{62} - 1$  and  $m_2 = 2^{62} - 3$ , which allowed us to represent  $p_n$  correctly. The NCI cluster is a heavily used shared computing facility so our major constraint was CPU time rather than memory. For this reason we chose to perform the calculation for all  $m_i$  in the same

**Table 2.** The number,  $p_n$ , of embeddings of  $n$ -step self-avoiding polygons on the square lattice. Only non-zero terms are listed.

$n$	$p_n$
112	646414111975777272517734370762400697757978
114	4304591798055577073477026735313861700713176
116	28687064652813390269800415016181829385121162
118	191320663411431818964849556990106874938907548
120	1276875276296096391140817393830149918943464494
122	8527773411790633004325737459634720668141188468
124	56991966408991589554333823232058663722205631080
126	381130017241685467740337492217602004487643160168
128	2550382601811089051031712642200910692143744745034
130	17076613429289025223970687974244417384681143572320

run. Effectively this doubles the memory requirement but only results in an increase in running time of some 15% (compared to a run using a single  $m_i$ ), that is, an overall *decrease* in total running time by a factor of about 2.6.

Table 2 lists the new terms obtained in this work for the number of polygons with perimeter 112–130. The number of polygons of length  $\leq 56$  can be found in [13] while those up to length 90 are listed in [10] and those to length 110 in [12]. The full series is available at [www.ms.unimelb.edu.au/~iwan](http://www.ms.unimelb.edu.au/~iwan).

### 3.1. Resource use

One of the main ways of achieving a good parallel algorithm using data decomposition is to try to find an invariant under the operation of the updating rules. That is we seek to find some property about the configurations along the boundary line which does not alter in a single iteration. The algorithm for the enumeration of polygons is quite complicated since not all possible configurations occur due to pruning, and the insertion of a new loop can change the state of an edge far removed. However, there still is an invariant since any edge not directly involved in the update cannot change from being empty to being occupied and vice versa. That is only the kink edges can change their occupation status. This invariant allows us to parallelise the algorithm in such a way that we can do the calculation completely independently on each processor with just two redistributions of the data set each time an extra column is added to the lattice. Since the number of processors we have to use is quite large (up to 1000) we actually did 3 redistribution per column. This increases the length of the invariant part and thus gives us better opportunities to ensure a decent load balance. We refer to [12] for details regarding the details of our parallelised implementation.

In Table 3 we have listed the main resources used by the parallel algorithm in order

**Table 3.** The resources used to calculate the number of SAP on rectangles of width  $w$ . Listed from left to right are the number of processors, the total CPU time in hours, the minimal and maximal number of configurations and series terms retained and finally the minimal and maximal time (in seconds) used in the redistribution. The minimum and maximum is taken across all of the processors.

$W$	Procs	Time	Min Conf	Max Conf	Min Term	Max Term	$t$ -min	$t$ -max
23	160	241	9950148	11503231	73828085	87381144	560	1436
24	400	557	8890870	9165975	56728718	61006162	699	763
25	592	1125	11962488	12287159	64909908	67080631	964	1096
26	800	2214	15923256	16383084	70084896	72376608	1345	1575
27	800	3713	24966483	25822571	87087766	90763851	2321	2650
28	1000	5559	26089184	26581112	71874712	73445360	2272	2730
29	800	4953	31025188	32021460	63918962	66526222	2379	2760
30	400	2874	34573073	35446404	52929622	54330414	2690	2926
31	96	450	25632787	26124867	31132604	31768765	1482	1588

to enumerate SAP up to perimeter 130. For each width  $W$  we first list the number of processors used and the total CPU time in hours required to complete the calculation for a given width. One of the main issues in parallel computing is that of load balancing, that is, we wish to ensure to the greatest extent possible that the workload is shared equally among all the processors. This aspect is examined via the numbers in columns 4–9. At any given time during the calculation each processor handles a subset of the total number of configurations. For each processor we monitor the maximal number of configurations and terms retained in the generating functions. Note that the number of terms listed is per modulo  $m_i$ ; so in total three times this number is actually stored. The load balancing can be roughly gauged by looking at the largest (Max Conf) and smallest (Min Conf) maximal number of configurations handled by individual processors during the execution of the program. In columns 6 and 7 are listed the largest (Max Term) and smallest (Min Term) maximal number of terms retained in the generating functions associated with the subset of configurations. As can be seen the algorithm is very well balanced. Finally in columns 8 and 9 we have listed the minimal and maximal total time (in seconds) spent by any processor in the redistribution part of the algorithm and as can be seen this part of the algorithm takes a total of some 15% of the CPU time. Note that most of this time is spent preparing for the redistribution and processing the data after it has been moved. The actual time spent in the MPI message passing routines is less than 5% of total CPU time.

#### 4. Series analysis and results

To obtain the singularity structure of the generating functions we used the numerical method of differential approximants [14]. We will not describe the method here and refer the interested reader to [14] for details, and Chapter 8 of [3] for an overview of

the method. Since all odd terms in the series are zero and the first non-zero term is  $p_4$  we actually analysed the series  $F(x) = \sum p_{2n+4}u^n$ . This function has a critical point at  $u = x_c^2$  with the same exponent as that of (2). In Table 4 we list estimates for the critical point  $x_c^2$  and exponent  $2 - \alpha$ . The estimates were obtained by averaging values obtained from second and third order differential approximants. For each order  $L$  of the inhomogeneous polynomial we averaged over those approximants to the series which used at least the first 55 terms of the series (that is, polygons of perimeter at least 110). The quoted error for these estimates reflects the spread (basically one standard deviation) among the approximants. Note that these error bounds should *not* be viewed as a measure of the true error as they cannot include possible systematic sources of error. Based on these estimates we conclude that  $x_c^2 = 0.143680629269(2)$  and  $\alpha = 0.500000015(20)$ .

Some years ago [15] it was pointed out that the polynomial  $581x^4 + 7x^2 - 13$  is the only polynomial with “small” integer coefficients for which the relevant zero  $x_0^2 = 0.1436806292698685\dots$  is consistent with the estimate for  $x_c$ . Clearly, with almost 12 digit accuracy the conjectured value still stands. It should be emphasised that there is no theoretical motivation for the conjecture. However, the agreement with the numerical estimate is very impressive (and perhaps surprising). In any case the polynomial can at least serve as a useful memory aid for  $x_c$ .

**Table 4.** Estimates for the critical point  $u_c^2$  and exponent  $2 - \alpha$  obtained from second and third order differential approximants to the series for square lattice polygon generating function.  $L$  is the order of the inhomogeneous polynomial.

$L$	Second order DA		Third order DA	
	$u_c^2$	$2 - \alpha$	$u_c^2$	$2 - \alpha$
0	0.1436806292669(38)	1.500000027(19)	0.1436806292683(18)	1.500000023(10)
2	0.1436806292697(35)	1.500000021(71)	0.1436806292690(12)	1.500000021(25)
4	0.1436806292684(16)	1.500000023(14)	0.1436806292694(11)	1.5000000155(66)
6	0.1436806292688(18)	1.500000019(11)	0.14368062926979(89)	1.5000000131(61)
8	0.1436806292684(18)	1.500000018(12)	0.1436806292699(15)	1.500000013(10)
10	0.1436806292686(16)	1.500000019(12)	0.1436806292695(11)	1.5000000154(68)

To gauge whether or not the estimates truly are as well converged as the results in Table 4 would suggest we find it useful to plot the actual individual estimates against  $n$  (where  $p_n$  is the last terms used to form a given differential approximant). In the first two panels of Figure 7 we have plotted the estimates for  $x_c^2$  and  $2 - \alpha$  as functions of  $n$ . Each point represents an estimate from a third order differential approximant. The approximants appear very well converged and given the very high resolution of the abscissa there is no sign of any significant systematic drift. Finally, in the third panel we plotted the estimated for  $2 - \alpha$  versus the corresponding estimates for  $x_c^2$ . If the conjectures for the exact values are correct the estimates should ideally pass through the point of intersection between the conjectured values. Clearly there is a very slight

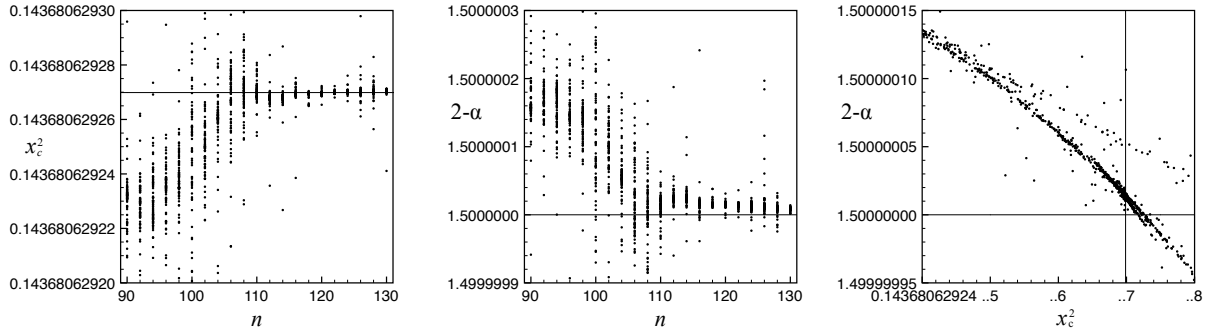


**Figure 7.** Estimates of the critical point  $x_c^2$  and critical exponent  $2 - \alpha$  versus  $n$  (left and middle panels) and  $2 - \alpha$  versus  $x_c^2$  (right panel) for the square lattice polygon generating function. The straight lines correspond to  $2 - \alpha = 3/2$  and  $x_c^2 = 0.1436806292698685 \dots$

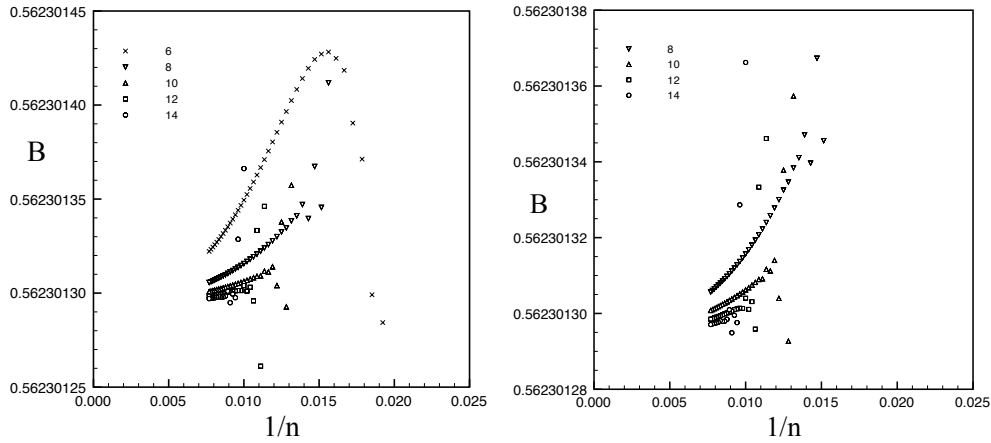


**Figure 8.** Estimates for the amplitude  $B$  versus  $1/n$ . Each data set is obtained by fitting  $p_n$  to the form (4) using from 6 to 14 correction terms. The plot on the right is an enlarged version of the plot to the left.

discrepancy here and for  $2 - \alpha = 3/2$  the ‘biased’ estimate for the critical point is  $x_c^2 = 0.1436806292672(1)$ . Since the difference only occurs in the 12<sup>th</sup> significant digit we do not feel confident that the numerical evidence alone is sufficient to settle the matter. Ultimately we will let the reader make their own judgement.

The detailed asymptotic form of the coefficients  $p_n$  of the polygon generating function has been studied in detail previously [16, 10, 12]. As argued in [16] there is no sign of non-analytic corrections-to-scaling exponents to the polygon generating function and one therefore finds that

$$p_n = \mu^n n^{-5/2} \sum_{i \geq 0} a_i/n^i, \quad \text{for } n \text{ even.} \quad (4)$$

Estimates for the leading amplitude  $B = a_0$  can thus be obtained by fitting  $p_n$  to the form (4) using increasing values of  $k$ . It is useful to check the behaviour of the estimates by plotting the results for the leading amplitude versus  $1/n$  (see Figure 8), where  $p_n$

is the last term used in the fitting, and  $n$  is varied from 130 down to 50. Note that as more and more correction terms are added the estimates exhibit less curvature and the slope become less steep. This is very strong evidence that (4) is indeed the correct asymptotic form of  $p_n$ . We estimate that  $B = 0.56230129(1)$ .

## 5. Summary and Outlook

We have implemented a new algorithm for the enumeration of SAP on the square lattice; the new method shows considerable promise for future enumeration studies. The new algorithm was used to extend the series for the number of SAP on the square lattice from  $n = 110$  to  $n = 130$ . Our analysis of the extended series yielded improved estimates of critical parameters:  $x_c^2 = 0.143680629269(2)$  ( $\mu = 2.63815853035(2)$ ),  $\alpha = 0.500000015(20)$ , and  $B = 0.56230129(1)$ .

We expect that the new algorithm will prove to be widely applicable. We chose SAP on the square lattice for this study because it is the simplest model for computer implementation and thus best for illustrating the basic principles involved and the differences between the old and new algorithms. The improvement in running time of some 15% while significant is unspectacular. However, we anticipate that the gains realised by the new algorithm will be greater for other lattices, and other models such as self-avoiding walks, theta graphs, and star polymers. It will be especially useful in situations where many candidate completions must be considered while pruning. This is certainly the case for three-dimensional lattices, for which the restrictions on crossing of nested loops do not exist, and we are hopeful that the new algorithm will allow for fast enumeration of three-dimensional lattice objects via the finite lattice method. In future, we will test this by implementing the new algorithm for SAP and SAW on the simple cubic lattice.

## Acknowledgements

This work was supported by an award under the Merit Allocation Scheme on the NCI National Facility at the ANU. NC was supported by the ARC Centre of Excellence for Mathematics and Statistics of Complex Systems (MASCOS). IJ was supported under the Australian Research Council's Discovery Projects funding scheme by the grant DP0770705.

## References

- [1] Madras N and Slade G 1993 *The self-avoiding walk* (Boston: Birkhäuser)
- [2] Hughes B D 1995 *Random Walks and Random Environments, Vol I Random Walks* (Oxford: Clarendon)
- [3] Guttmann A J, ed. 2009 *Polygons, Polyominoes and Polycubes* vol. 775 of *Lecture Notes in Physics* (Springer)
- [4] Leibler S, Singh R R P and Fisher M E 1987 Thermodynamic behavior of two-dimensional vesicles *Physical Review Letters* **59** 1989–1992



- [5] Fisher M E 1989 Fractal and nonfractal shapes in two-dimensional vesicles *Physica D* **38** 112–118
- [6] Fisher M E, Guttman A J and Whittington S G 1991 Two-dimensional lattice vesicles and polygons *Journal of Physics A* **24** 3095–3106
- [7] Nienhuis B 1982 Exact critical point and critical exponents of  $O(n)$  models in two dimensions *Physical Review Letters* **49** 1062–1065
- [8] Nienhuis B 1984 Critical behavior of two-dimensional spin models and charge asymmetry in the Coulomb gas *Journal of Statistical Physics* **34** 731–761
- [9] Enting I G 1980 Generating functions for enumerating self-avoiding rings on the square lattice *J. Phys. A* **13** 3713–3722
- [10] Jensen I and Guttman A J 1999 Self-avoiding polygons on the square lattice *J. Phys. A* **32** 4867–4876
- [11] Guttman A J and Whittington S G 1978 Two-dimensional lattice embeddings of connected graphs of cyclomatic index two *Journal of Physics A: Mathematical and General* **11** 721–729
- [12] Jensen I 2003 A parallel algorithm for the enumeration of self-avoiding polygons on the square lattice *J. Phys. A* **36** 5731–5745
- [13] Guttman A J and Enting I G 1988 The size and number of rings on the square lattice *Journal of Physics A* **21** L165–172
- [14] Guttman A J 1989 Asymptotic analysis of power-series expansions in *Phase Transitions and Critical Phenomena* (eds. C Domb and J L Lebowitz) (New York: Academic) Vol. 13 1–234
- [15] Conway A R, Enting I G and Guttman A J 1993 Algebraic techniques for enumerating self-avoiding walks on the square lattice *J. Phys. A: Math. Gen.* **26** 1519–1534
- [16] Conway A R and Guttman A J 1996 Square lattice self-avoiding walks and corrections to scaling *Phys. Rev. Lett.* **77** 5284–5287